National Defence / Défense nationale

UNCLASSIFIED
UNLIMITED DISTRIBUTION

DREV REPORT 4653/91
AUGUST 1991

CRDV RAPPORT 4653/91
AOÛT 1991

A PROCEDURE FOR OBTAINING AN ALGEBRAIC APPROXIMATION TO CERTAIN INTEGRALS

B.T.N. Evans

G.R. Fournier

RESEARCH AND DEVELOPMENT BRANCH
DEPARTMENT OF NATIONAL DEFENCE
CANADA

BUREAU - RECHERCHE ET DÉVELOPPEMENT
MINISTÈRE DE LA DÉFENSE NATIONALE
CANADA

Defence Research Establishment
Centre de recherches pour la Défense
Valcartier, Quebec

Canada

SANS CLASSIFICATION
DISTRIBUTION ILLIMITÉE

DREV R-4653/91 UNCLASSIFIED CRDV R-4653/91

A PROCEDURE FOR OBTAINING AN ALGEBRAIC APPROXIMATION TO CERTAIN INTEGRALS

by

B.T.N. Evans and G.R. Fournier

DEFENCE RESEARCH ESTABLISHMENT

CENTRE DE RECHERCHES POUR LA DÉFENSE

VALCARTIER

Tel: (418) 844-4271

Québec, Canada August/août 1991

SANS CLASSIFICATION

ABSTRACT

We have found a method for obtaining algebraic approximations to certain integrals that appears to be independent of known methods, such as Taylor, orthonormal functions, Laplace's method, etc. This method has the advantage of sometimes producing much more compact forms of the integral. It often gives results where the others may fail and in many cases the solutions are globally valid over the full range of each parameter. It sometimes allows for a trade-off between the accuracy and the functional complexity of the solution.

Specific problems in the estimation of extinction from obscurants and other aerosols are for the first time completely resolved analytically. These analytical solutions are applicable to infrared and millimeter wave smokes as well as biological and natural aerosols.

RÉSUMÉ

Nous avons trouvé une méthode qui permet d'obtenir des approximations algébriques à certaines intégrales. Cette méthode nous apparaît indépendante des autres méthodes connues comme celle de Taylor, de Laplace, ou celle des expansions en fonctions orthonormales. Dans certains cas, cette méthode a l'avantage de produire des formes beaucoup plus compactes de l'intégrale, de donner un résultat alors que les autres méthodes échouent et de produire des solutions globalement valides sur toute l'échelle des valeurs de chaque paramètre. Elle permet souvent de balancer la précision du résultat et la complexité fonctionnelle de la solution.

Certains problèmes qui concernent l'extinction causée par les agents obscurcissants et par les aérosols ont été complètement solutionnés analytiquement pour la première fois. Ces solutions analytiques sont applicables aux fumées actives dans les régions infrarouges et millimétriques ainsi qu'aux aérosols d'origine biologique et naturelle.

TABLE OF CONTENTS

EXECUTIVE SUMMARY

Any complex military system or scenario that involves electro-optics requires the solution to one or many diffraction problems. This includes propagation of radiation through natural aerosols, smokes/obscurants, design and evaluation of high precision optical systems, novel laser cavities, etc.

Diffraction problems nearly always involve the evaluation of a certain class of integrals. These integrals are usually intractable and thus must be computed numerically. Hence, this can be not only computationally expensive but there is in general, significant loss of physical understanding.

This report describes a technique that, for many diffraction-type integrals, gives an approximate but efficient analytic solution. This reduces the computational effort considerably while retaining the physical insight essential for system design or scenario analysis.

Specific integrals involved in the estimation of extinction from obscurants and other aerosols are for the first time completely resolved analytically. These analytical solutions are applicable to infrared and millimeter wave smokes as well as to biological and natural aerosols.

Although all examples given in this work originate from the diffraction of electromagnetic radiation by aerosols, the integration technique is not necessarily restricted to this area of physics. We therefore expect the technique to be useful in other fields. It is at this stage a possible solution looking for other promising problems.

1.0 INTRODUCTION

There are some areas in physics where an analytic approximation to an integral is highly desirable even though it is inexact. This is particularly true when the physical theory is known to be only an approximation itself. A striking example are integrals that occur in the Fresnel-Huygens or Kirchhoff form of scalar diffraction theory which is applicable to both optics and acoustics. Aerosol scattering problems provide another example. One wishes for an approximate analytic solution in order to retain at least one of the following: physical insight, correct asymptotic behaviour, computational speed and/or computational robustness.

We have found a method for obtaining algebraic approximations to certain integrals that appears to be independent of known methods, such as Taylor, orthonormal functions, method of stationary phases, steepest descent, etc. This method has the advantage of often producing much more compact forms of the integral and sometimes producing results where the others may fail. It sometimes allows for a trade-off between the accuracy and the functional complexity of the solution. For the practical purposes of this report, when we refer to an analytic solution we mean that the result of integration must be represented in terms of combinations of the elementary and special functions of mathematical physics.

The integrals that can be approximated by this method are the same as those found in integral tables but the arguments of some of the functions in the kernel are much more complicated. As will be shown, the main limitation of the technique is that there is no *a*

priori error estimation nor is the method as yet fully automated.

This work was performed at DREV between July and December 1990 under PSC 32A, EO/IR Protection of Land Vehicles.

2.0 METHOD

This chapter gives the general mathematical framework required to implement the integration technique.

2.1 Outline of Concept

Suppose one has the following integral to perform:

$$I = \int_a^b g(\lambda_i, h(\eta_j, x))\, f(\sigma_k, x)\, dx \qquad [1]$$

where g, h and f are any continuously differentiable functions and λ_i, η_j and σ_k are parameters independent of x whose domain can cover, in general, the complex plane. In order to refer to the whole set of parameters we will define $p = \{\lambda_i, \eta_j, \sigma_k\}$. As it stands, [1] is a general integral with a function that has a potentially very complicated argument $h(\eta_j, x)$. Most integrals that have analytic solutions have rather simple arguments. The following method extends the list of analytically soluble integrals to a list that includes analytically approximated integrals.

We start off by assuming that a function $u(q_l, h)$ can be found such that

$$\int_{h(\eta_j,a)}^{h(\eta_j,y)} u(q_l,h)\,dh \approx \int_a^y f(\sigma_k,x)\,dx \qquad [2]$$

is an acceptable approximation valid over the range of integration. Here y ranges between a and b, and the q_l are n fitting parameters. The number of fitting parameters n will generally depend on the functional form chosen for u. We next apply Leibniz's theorem for differentiation of an integral on [2] to get:

$$\begin{aligned} \frac{d}{dy}\int_{h(\eta_j,a)}^{h(\eta_j,y)} u(q_l,h)\,dh &\approx \frac{d}{dy}\int_a^y f(\sigma_k,x)\,dx \quad \text{which gives} \\ u(q_l,h(y))\,dh &\approx f(\sigma_k,y)\,dy. \end{aligned} \qquad [3]$$

Multiplying each side of [3] by $g(h)$ and integrating we get:

$$I \approx \int_\alpha^\beta g(h)\,u(h)\,dh \qquad [4]$$

where $\alpha = h(\eta_j, a)$ and $\beta = h(\eta_j, b)$ to simplify the notation. Whether [2] is an acceptable approximation will depend on the desired accuracy of [4].

It is required that [4] be analytically integrable. It is often preferable, but not necessary, that both the integrals in [2] also be analytically integrable. It is clear that when the approximation [2] is exact this procedure is just a variable substitution.

Equation [2] can be further generalized to

$$\int_\alpha^\beta \sum_k a_k\,u_k(q_{lk},h)\,dh \approx \int_a^y f(\sigma_k,x)\,dx, \qquad [5]$$

with a_k weighting constants, keeping in mind that for each k

$$\int_{\alpha}^{\beta} g(h)\, u_k(h)\, dh \qquad [6]$$

must be analytically integrable. Thus for each function, u_k, that satisfies the integrability conditions in [6], an additional functional form is found that may improve the approximation in [5].

The concept above will be made clearer by an outline of some possible procedures and several examples taken from actual physical problems.

2.2 Outline of a Procedure

In the following subsections we will outline the steps of one procedure for putting into practice the previous concept.

2.2.1 Finding Candidate u

In deriving a practical procedure for implementing the above method, it is useful to prune the set of possible forms of u. The strongest constraint is the integrability condition [4] or [5]. One way of determining part of the allowed set of functional forms for u is by looking up a table of definite integrals that contain products of g and other functions. A more general way is to consider the small list of general integrals (Refs. 1-4). This list can be used to rapidly survey almost all known analytic definite integrals. Although these

integrals are complicated, they, at the very least, serve as indicators as to the existence of possible forms of u. Examples from this list, two of which we will use, are given below.

$$\int_0^1 x^{\rho-1}(1-x)^{\beta-\nu-u}\,{}_2F_1(-u,\beta;\nu;x)\,G_{p,q}^{m,n}\left(z\,x^s\middle|\begin{matrix}a_1, & \ldots, & a_p\\ b_1, & \ldots, & b_q\end{matrix}\right)dx$$
$$= \frac{\Gamma(\nu)\Gamma(\beta+1-\nu)\,s^{u+\nu-\beta-1}}{\Gamma(\nu+u)}G_{p+2s,q+2s}^{m+s,n+s}\left(z\middle|\begin{matrix}g_s, & a_1, & \ldots, & a_p, & h_s\\ i_s, & b_1, & \ldots, & b_q, & j_s\end{matrix}\right) \qquad [7]$$

$$\int_1^\infty x^{-\rho}(x-1)^{\sigma}\,{}_2F_1(\kappa+\sigma-\rho,\lambda+\sigma-\rho;\sigma;1-x)\,G_{p,q}^{m,n}\left(z\,x\middle|\begin{matrix}a_1, & \ldots, & a_p\\ b_1, & \ldots, & b_q\end{matrix}\right)dx$$
$$= \Gamma(\sigma)G_{p+2,q+2}^{m+2,n}\left(z\middle|\begin{matrix}a_1, & \ldots, & a_p, & \kappa+\sigma-\rho, & \rho\\ \kappa, & \lambda, & b_1, & \ldots, & b_q\end{matrix}\right) \qquad [8]$$

$$\int_0^1 x^{\sigma-1}(1-x)^{\rho-1}\,F_{C:D;D'}^{A:B;B'}\left(\begin{matrix}(a): & (b); & (b')\\ (c): & (d); & (d')\end{matrix}\middle|\alpha x^m(1-x)^n,\beta x^m(1-x)^n\right)dx$$
$$= \frac{\Gamma(\sigma)\,\Gamma(\rho)}{\Gamma(\sigma+\rho)}F_{C+m+n:D;D'}^{A+m+n:B;B'}\left(\begin{matrix}(a), & \frac{\sigma}{m}, & \ldots, & \frac{\sigma+m-1}{m}, & \frac{\rho}{n}, & \ldots, & \frac{\rho+n-1}{n}\\ (c), & \frac{\sigma+\rho}{m+n}, & \ldots, & \ldots, & \ldots, & \ldots, & \frac{\sigma+\rho+m+n-1}{m+n}\end{matrix}\right.\ :$$
$$\left.\begin{matrix}(b); & (b')\\ (d); & (d')\end{matrix}\middle|\frac{m^m\alpha}{(m+n)^{m+n}},\frac{n^n\beta}{(m+n)^{m+n}}\right). \qquad [9]$$

Equations [7] and [9] are examples of general Euler type integrals. In [7], ${}_2F_1$ is the Gauss hypergeometric function and $G_{p,q}^{m,n}$ is Meijer's G-function. In [9] $F_{C:D;D'}^{A:B;B'}$ is a Kampé de Fériet function. This double variable hypergeometric function and its properties are discussed at length in (Ref. 5) and more recently in (Ref. 4). One very important property of the Kampé de Fériet functions, that we will use in an example, occurs when C and A are both zero in which case they become just the product of two generalized hypergeometric functions of a single variable:

$$F_{0:D;D'}^{0:B;B'}\left(\begin{matrix}(a): & (b); & (b')\\ (c): & (d); & (d')\end{matrix}\middle|x,y\right) = {}_BF_D\left(\begin{matrix}(b)\\ (d)\end{matrix}\middle|x\right)\,{}_{B'}F_{D'}\left(\begin{matrix}(b')\\ (d')\end{matrix}\middle|y\right). \qquad [10]$$

Equation [8] is a general Weyl integral over the product of a Gauss hypergeometric function and a Meijer's G-function. The detailed conditions of validity of these integrals will not be stated here so as not to sidetrack the main issues. They can however be found in the cited references.

With these integrals the functions g and u, plus the appropriate integral transform can be identified. Hence g or u could be either a Meijer's G-function, a generalized hypergeometric function, simple functions (such as x^ρ, $(1-x)^\mu$, e^x or $\sin(x)$), etc. Thus most functions occurring in mathematical physics are covered.

Additional qualitative considerations of the functional form of the right-hand side of [2] can further reduce the set of candidate forms for u. Some of the more obvious ones are the monotonicity, curvature and asymptotic behavior in both large and small limits. A more subtle condition is the weighting provided by g in [4].

2.2.2 Obtaining the Fitting Parameters q_l

The fitting parameters, q_l (in general, but not always, functions of p, a and b), in [2] are obtained by some appropriate minimizing procedure that reduces the error in the approximation [4]. This can be stated in one form as:

$$\text{Min}\left| \int_a^b \left\{ \int_{h(\eta,a)}^{h(\eta,x)} g(h)\, u(q_l, h)\, dh - \int_a^x g(h(x))\, f(x)\, dx \right\} dy \right| \qquad [11]$$

where the Min is understood to be performed for a particular set of p. The process is repeated over the parametric space of interest in p. If the level of error is not satisfactory, another candidate form for u must be tried either in [2] or [5]. In the latter case, we note that fitting of a_k is also required.

Possible minimizing strategies could include numerical methods such as quasi-Newton, conjugate gradient or simplex, etc. These methods initially do not produce analytic expressions of q_l in terms of h, p, a and b. However, provided that the dependency is not too complicated, acceptable functional approximations may be found.

The above process is complicated, can be computationally demanding and ultimately could be intractable. However, the examples in the next chapter show that often the situation can be considerably simplified by relaxing the constraint equation [11]. Indeed it will be shown that even a trial and error method for finding u can often suffice. The constraint condition [11] is also reduced by first assuming that g is a constant, and then fitting at only a small set of points, y_l, equal to the number of fitting parameters n. Thus [11] becomes

$$\left| \int_{h(\eta_j,a)}^{h(\eta_j,y_l)} u(q_l,h)\,dh - \int_a^{y_l} f(x)\,dx \right| = 0, \quad l = 1,2,\ldots n \qquad [12]$$

The function g is only peripherally considered when choosing y_l and u. As will be shown by examples, [12] sometimes can be solved analytically, i.e. q_l in terms of h, p, a and b. This simplified procedure has been shown to work for functions with simple forms such as monotonic ones, whose curvature is easily modelled.

3.0 EXAMPLES

In this chapter we will give several examples of the application of the method to various integrals that occur in optical scattering theory. None of these can be transformed into integrals that have closed form solutions in terms of special functions. Moreover, since the parameters in each kernel can arbitrarily take on values from 0 to ∞, Taylor series expansions and asymptotic methods such as Laplace's or steepest descents will not work because of convergence problems. Since part of the kernel has a complicated argument, any expansion in sets of orthogonal functions will also involve this argument and hence will most likely make any possible solution undesirable. In all three cases, the solution obtained is valid globally over the complete range of each parameter in $\wp$. This last point will be illustrated by extensive tables.

3.1 Example 1

The following example occurs in the study of scalar scattering from randomly oriented infinite aspect discs.

$$Q_d = 2(1 - \mathrm{Re}(I_d)) \quad \text{with}$$

$$I_d = \int_0^1 e^{-\omega(x)} dx \qquad [13]$$

where $\omega(x) = 2is[(m^2 - x)^{1/2} - (1 - x)^{1/2}]$, s is the particle size parameter, a real number varying between 0 and ∞, and m is the refractive index and is hence complex with $\mathrm{Re}(m)$

varying between 1 and ∞ and $\mathrm{Im}(m)$ varying between 0 and $-\infty$. Hence the magnitude of $\omega(x)$ varies from 0 to ∞ as well.

Following the notation of the previous chapter, $h(\eta_1, \eta_2, x) = \omega$, $g(h) = e^{-h}$, $f(x) = 1$, $a = 0$, and $b = 1$. The parameters are obviously $\eta_1 = s$ and $\eta_2 = m$ and thus $\wp = \{\eta_1, \eta_2\}$.

The functional form of u is constrained by the integrability condition [4]. As $g(h) = e^{-h}$, the simplest nontrivial possible forms of $u(h)$ are limited to ce^{-dh} or $1/(h+c)^d$ where c and d are constants. The term "simplest" is defined here by the order of the hypergeometric function used. For these forms e^h is a ${}_0F_0$ and $1/(h+c)$ is a ${}_1F_0$, all other hypergeometric functions are much more complicated in their behavior, computation and in the integrals that would result from this procedure. Of the two forms identified above, ce^{-dh} gives rise to a set of transcendental equations that needs to be solved in order to obtain c and d. We thus choose the form $1/(h+c)^d$ which produces readily solvable equations. This form gives the approximation of I in terms of exponential integrals of order d.

Let

$$J(y_l) \equiv \int_0^{y_l} f(x)\,dx = y_l. \qquad [14]$$

Since, over the range of physical interest $\mathrm{Re}(m) > 1$, h is a simply behaved function of y_l, we can find, in this case, a transformation relating h to J. Here, this transformation u can be of the form stated above. Thus we have

$$\int u(h)\,dh \propto \int \frac{dh}{(h+c)^d} \propto \frac{1}{(h+c)^{(d-1)}}. \qquad [15]$$

We have empirically found that $d = 2$ is a reasonably good approximation to J. Furthermore since the above form allows a maximum of three fitting parameters, $n = 3$.

Thus we find

$$J(y_l) = y_l \approx \frac{q_1}{h(y_l) + q_2} + q_3, \quad l = 1, 2, 3. \tag{16}$$

This set of equations can be expressed as three linear equations which are readily solved for q_l. The values of y_l were chosen so that the equations are simple, i.e. $y_1 = 0$, $y_2 = 1/2$ and $y_3 = 1$. Other sets of y_l could be used achieving a slightly better approximation at the expense of algebraic complexity. With the chosen set of y_l, the solution to [16] is

$$\begin{aligned} q_1 &= -(h(0) + q_2)q_3 \\ q_2 &= \frac{h(0)h(1/2) - 2h(0)h(1) + h(1/2)h(1)}{h(0) - 2h(1/2) + h(1)} \\ q_3 &= \frac{h(1) + q_2}{h(1) - h(0)}. \end{aligned} \tag{17}$$

In the above we have simplified the notation for $h(\eta_1, \eta_2, y_l)$ to $h(y_l)$ for clarity.

With the above equations we can substitute into [4] to get:

$$\begin{aligned} I_d &\approx -q \cdot \int_{h(0)}^{h(1)} \frac{e^{-h}}{(h + q_2)^2} dh \\ &= q_1 e^{q_2} \left[\frac{E_2(h(1) + q_2)}{h(1) + q_2} - \frac{E_2(h(0) + q_2)}{h(0) + q_2} \right]. \end{aligned} \tag{18}$$

Note that E_2 is the second order exponential integral. Thus the integral [13] has been approximated as the difference of two second order exponential integrals.

Table I presents a comparison between the exact numerical calculation of I_d and the approximation [18].

As seen in Table I, when the magnitude of I_d is significant the percent error is relatively small. However, when the magnitude of I_d approaches 0 the percent error can be quite large. The latter effect is due to an error in the phase of the approximation with respect to the exact solution. This effect will occur when the approximation does not have the same zero crossings as the exact integral. This applies to any approximation technique and is therefore not specific to the present procedure. Note that where the approximation is matched at a zero, i.e. at infinite refractive index, the percent error is small. Evidently matching one or more zeros of the integral could be a useful criterion in the choice of an adequate form of h. However, in the present case the quantity of physical interest is Q_d and thus, whenever I_d is small the percent error in Q_d will be also small. For example, for the worst case in Table I, $m = 2.0$ and $s = 5$, where the error in I_d is 103.7%, the corresponding percent error in Q_d is only 11.0%.

3.2 Example 2

The integral in this example is taken from (Ref. 6) and, as in the previous example, occurs in the scalar theory of electromagnetic and acoustic scattering. This integral accounts for the effect of edge scattering from randomly oriented prolate spheroids of arbitrary aspect

TABLE I

Error table for Example 1

m	s	I_d Exact	I_d Approximation	—% Error—
1.1	.001	1-.000312902i	1-.000331086i	0,5.8
1.1	.01	.999994-.00313015i	.999993-.00331084i	.0001,5.8
1.1	.1	.999439-.0312943i	.999337-.0330977i	.01,5.8
1.1	1	.944813-.305286i	.935227-.320415i	1.0,5.0
1.1	2	.790095-.566587i	.758557-.581541i	4.0,2.6
1.1	5	.0551996-.849220i	.0305116-.781481i	44.7,8.0
1.1	10	-.592805-.237394i	-.540190-.272222i	8.9,14.7
1.1	50	.0609117+.197822i	.0487599+.217617i	19.9,10.0
1.1	100	-.0911145-.0580755i	-.0989528-.0729561i	8.6,25.6
1.5	1	.258516-.932335i	.226920-.925756i	12.2,0.7
1.5	2	-.743586-.465533i	-.719633-.407902i	3.2,12.4
1.5	5	.490254+.09049i	.416438+.162019i	15.1,79.0
1.5	10	.0836259+.269668i	.0418624+.276025i	49.9,2.4
1.5	50	.0192536-.0568162i	.0215849-.0637607i	12.1,12.2
1.5	100	.0160325-.0253829i	.0183567-.0307823i	14.5,21.3
1.5-.01i	1	.25309-.911135i	.222336-.90455i	12.2,.72
1.5-.01i	10	.065439+.220519i	.0320381+.226246i	51.0, 2.6
1.5-.01i	100	.00221063-.00340189i	.00259562-.00402052i	17.4,18.2
1.5-.1i	1	.207354-.741218i	.183119-.734624i	11.7,.89
1.5-.1i	10	.00677562+.0353941i	.00220001+.0368946i	67.5,4.2
1.5-1i	1	.0183699-.107124i	.0152086-.014582i	17.2,2.4
2.0	1	-.700659-.641335i	-.706793-.603780i	.88,5.9
2.0	2	.0469974+.813015i	.0734549+.743366i	56.3,8.6
2.0	5	.0958382+.345685i	-.00351873+.373174i	103.7,8.0
2.0	10	-.158222-.109586i	-.164505-.162528i	4.0,48.3
2.0	50	.0216164-.0338167i	.0250502-.0426432i	15.9,26.1
2.0	100	.0175966-.00939819i	.0225043-.00950006i	27.9,1.1
35-35i	.001	.930190-.0639669i	.930189-.0640105i	.0001,.068
35-35i	.01	.384032-.314763i	.383882-.314941i	.04,.057
35-35i	.05	-.0289054+.00866923i	-.0288829+.00873602i	.08,.77
35-35i	.09	.00182362+.000190088i	.00182381+.000182345i	.01,4.1

ratio.

$$I_e = \int_0^{\pi/2} P \sin(\theta)\, e^{-c_0 (\frac{r}{P s})^{2/3}\, {}_2F_1[-\frac{2}{3},\frac{1}{2};1;1-\frac{1}{P^2}]}\, d\theta, \qquad [19]$$

where s, r and c_0 are constants and $P = [\cos^2(\theta) + r^2 \sin^2(\theta)]^{1/2}$. For this case r, the aspect ratio, can vary from 1 to ∞, s, again the size parameter, can vary from 0 to ∞ and the Fock constant, $c_0 \approx 1$.

Identify h with ${}_2F_1[-\frac{2}{3},\frac{1}{2};1;1-\frac{1}{P^2}]/P^{2/3}$, $g(\lambda_1, h)$ with $e^{\lambda_1 h}$, f with $P\sin(\theta)$, $a = 0$ and $b = \pi/2$. For the parameters we have $\lambda_1 = c_0 (r/s)^{\frac{2}{3}}$, and $\eta_1 = \sigma_1 = r$. Thus we have the simple set $\wp = \{\lambda_1, \eta_1\}$.

Let

$$\begin{aligned} J(y_l) &= \int_0^{y_l} P \sin(\theta)\, d\theta \\ &= \frac{r}{2}\left[\sqrt{1-\epsilon^2} + \frac{\sin^{-1}(\epsilon)}{\epsilon}\right] - \frac{r}{2}\left[\cos(y_l)\sqrt{1-\epsilon^2\cos^2(y_l)} + \frac{\sin^{-1}(\epsilon\cos(y_l))}{\epsilon}\right] \end{aligned}$$

and

$$\epsilon^2 = 1 - 1/r^2. \qquad [20]$$

Figure 1 is a plot of $h(\theta)$ and $J(\theta)$ versus θ for various values of r. These curves are very similar and it is evident that there should be a simple transformation that would take one function into the other.

We find $d = 2$ a reasonably good approximation to the curvature of J if we use the same functional form for u as in the previous example. As before, this form gives the

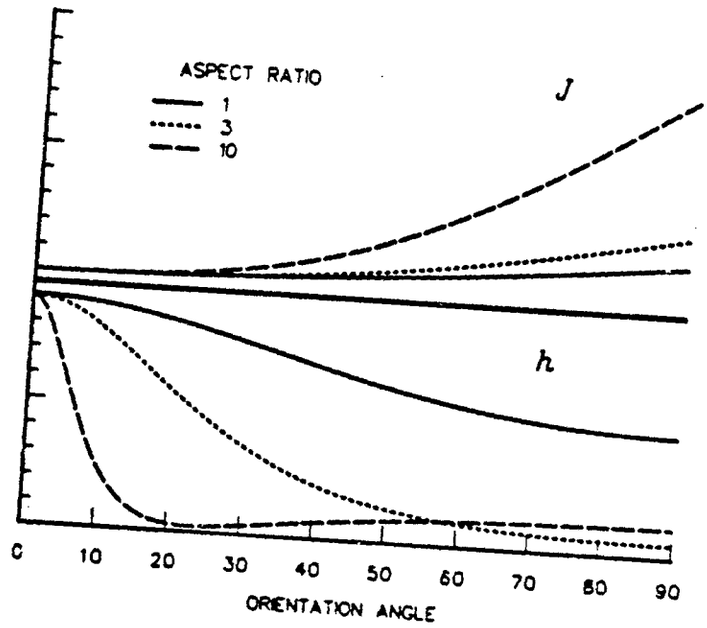

FIGURE 1 – A plot of $h(\theta)$ and $J(\theta)$ versus θ for various values of r (Example 2)

maximum number of three fitting parameters, i.e. $n = 3$. Thus, again we find

$$J(y_l) \approx \frac{q_1}{h(y_l) + q_2} + q_3, \quad l = 1, 2, 3. \tag{21}$$

As before, the values of y_l were chosen to keep the equations simple, i.e. $y_1 = 0$, $y_2 = \pi/4$ and $y_3 = \pi/2$. With the chosen set of y_l and using the fact that $h(0) = 1$, the solution to [21] is

$$\begin{aligned} q_1 &= \gamma q_3 [J(\pi/2) - q3] \\ q_2 &= \gamma q_3 - h(\pi/2) \\ q_3 &= \frac{h(\pi/2) - h(\pi/4)}{\gamma + [1 - h(\pi/4)]/J(\pi/4)} \\ \gamma &= \frac{h(\pi/2) - 1}{J(\pi/2)}. \end{aligned} \tag{22}$$

TABLE II

Error table for Example 2

r	s	I_e Exact	I_e Approximation	—% Error—
1	s	I_e	I_e	0
1.25	.01	3.65592×10^{-9}	3.10578×10^{-9}	15.05
1.25	.1	.0153844	.0149671	2.71
1.25	1	.456008	.453797	0.48
1.25	2	.645879	.643957	0.30
1.25	5	.847290	.845950	0.16
1.25	10	.954779	.953836	0.10
1.25	100	1.12007	1.11984	0.02
1.5	.01	1.92704×10^{-8}	1.57466×10^{-8}	18.29
1.5	.1	.0230733	.0222162	3.71
1.5	1	.549222	.545706	0.64
1.5	2	.764053	.761085	0.39
1.5	5	.989166	.987146	0.20
1.5	10	1.10846	1.10705	0.13
1.5	100	1.29101	1.29067	0.03
2.0	.01	1.45147×10^{-7}	1.20570×10^{-7}	16.9
2.0	.1	.0419768	.0404307	3.68
2.0	1	.745312	.740096	0.70
2.0	2	1.01026	1.00589	0.43
2.0	5	1.28302	1.28007	0.23
2.0	10	1.42612	1.42407	0.14
2.0	100	1.64362	1.64311	0.03
5.0	.01	3.89743×10^{-6}	3.61508×10^{-6}	7.24
5.0	.1	.385611	.380045	1.44
5.0	1	1.97382	1.95165	1.12
5.0	2	2.55329	2.53113	0.87
5.0	5	3.12749	3.10992	0.56
5.0	10	3.42199	3.40885	0.38
5.0	100	3.8627	3.85911	0.09

TABLE II (continued)

r	s	I_e Exact	I_e Approximation	—% Error—
10	.01	1.22907×10^{-5}	1.17944×10^{-5}	4.04
10	.1	.385611	.380045	1.44
10	1	4.02320	3.96007	1.57
10	2	5.14791	5.08044	1.31
10	5	6.24900	6.19179	0.92
10	10	6.80926	6.76488	0.65
10	100	7.64262	7.62982	0.17
100	.01	.00014741	.000144273	2.12
100	.1	4.03452	3.97989	1.35
100	1	40.6192	39.7725	2.08
100	2	51.7342	50.7669	1.87
100	5	62.5487	61.6353	1.46
100	10	68.0260	67.2530	1.14
100	100	76.1406	75.8643	0.36
10^4	.01	.0147756	.014492	1.92
10^4	1	4062.54	3974.18	2.17
10^4	100	7613.79	7576.89	0.48
10^5	.01	.147756	.144931	1.91
10^5	100	76137.9	75764.8	0.49
10^6	.01	1.47756	1.44923	1.92
10^6	100	761379.	757639.	0.49

With the above equations we can substitute into [4] to get:

$$I_e \approx q_1 \int_\alpha^\beta \frac{e^{-\lambda_1 h}}{(h+q_2)^2}\,dh$$

$$= e^{\lambda_1 q_2} q_1 \left[\frac{E_2(\lambda_1\alpha)}{\alpha} - \frac{E_2(\lambda_1\beta)}{\beta}\right] \quad \text{with} \qquad [23]$$

$$\alpha \equiv h(0) = 1$$

$$\beta \equiv h(\pi/2).$$

Table II presents the error between the exact numerically calculated value of I_e and [24] for a wide range of r and s values.

For an aspect ratio of 1, the approximation is equal to I_e exactly for any size parameter s. The error is greatest for a given r when s is small. This is once again due to the presence of a zero in the integral for $s = 0$. The approximation is exact (i.e., equal to 0) for $s = 0$, however the asymptotic behavior as s approaches 0 is not quite correct. This is not important for the physical problem of edge scattering since the real quantity of interest is related to $2 - I_e(s)/I_e(\infty)$.

3.3 Example 3

This example occurred in the study of scattering from randomly oriented infinite cylinders (Ref. 7).

$$I_c^1 = \int_0^{\pi/2} \mathbf{H}_1(w)\, \sin^2(\theta)\, d\theta \qquad [24]$$

where $\mathbf{H}_1$ is the first order Struve function and $w = 2s[(m^2 - \cos^2(\theta))^{1/2} - \sin(\theta)]$. The size parameter s can vary from 0 to ∞, $\mathrm{Re}(m)$ can vary from 1 to ∞, and $\mathrm{Im}(m)$ from 0 to $-\infty$. Again m is the index of refraction.

In this integral $h = w/2s$, $g(\lambda_1, h) = \mathbf{H}_1(\lambda_1 h)$, $f(\theta) = \sin^2(\theta)$, $a = 0$, and $b = \pi/2$. The parameters are $\lambda_1 = 2s$ and $\eta_1 = m$. Thus $p = \{\lambda_1, \eta_1\}$. Again the integrability condition [4] must be satisfied. Since $g(\lambda_1, h) = \mathbf{H}_1(\lambda_1 h) = {}_1F_2[1; 3/2, 5/2; -\lambda_1^2 h^2/4]$, we can transform [24] into an integral of a form similar to [9]. If we consider [10], the hypergeomet-

ric representation of H_1 as given above and in [9], then the choices for u will be "restricted" to a general hypergeometric ${}_pF_q$. However, since attention must be given to the computational feasibility of the solution, only the lowest order hypergeometric functions should be considered. Note also that the exponent of the variable h in the chosen hypergeometric function must be 2 in accordance with [9].

Let

$$\begin{aligned} J(y_l) &= \int_0^{y_l} \sin^2(\theta)\, d\theta \\ &= \frac{y_l}{2} - \frac{\cos(y_l)\sin(y_l)}{2}. \end{aligned} \qquad [25]$$

Figure 2 is a plot of $h(\theta)$ and $J(\theta)$ versus θ. Again as in the previous example, these curves are similar in that they are both monotonic with gentle curvature. Given the restrictions placed on u as detailed above, the simplest hypergeometric function that can be used is ${}_0F_0[;ch^2] = e^{ch^2}$. In this case the approximation to J would be

$$J(y_l) \approx q_1 \mathrm{Erf}[q_2 h(y_l)] + q_3, \quad l = 1,2,3. \qquad [26]$$

Choosing $y_1 = 0$, $y_2 = 1$ and $y_3 = \pi/2$ and solving for the fitting parameters we get:

$$\begin{aligned} q_1 &= \frac{-\pi/4}{\mathrm{Erf}[q_2 h(0)] - \mathrm{Erf}[q_2 h(\pi/2)]} \\ q_3 &= -q_1 \mathrm{Erf}[q_2 h(0)] \end{aligned} \qquad [27]$$

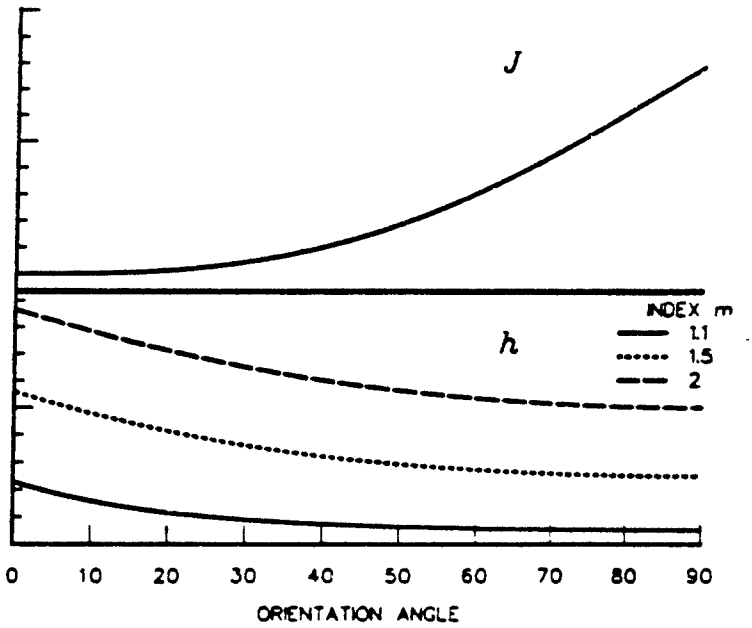

FIGURE 2 - A plot of $h(\theta)$ and $J(\theta)$ versus θ (Example 3)

and q_2 is the root of

$$\frac{\text{Erf}[q_2 h(0)] - \text{Erf}[q_2 h(1)]}{\text{Erf}[q_2 h(0)] - \text{Erf}[q_2 h(\pi/2)]} = \frac{4}{\pi} J(1). \qquad [28]$$

Here we have the situation where one of the fitting parameters, in this case q_2, cannot be solved for explicitly. We therefore must approximate the solution of [28] with some simple analytic function. This can be done by replacing the Erf functions in [28] with their first order asymptotic expansion. This is justified since it can be shown that $q_2 h(y_l)$ is always greater than 1.49. Doing this, we find that the limiting function, both for large and small Abs$(m-1)$ is:

$$q_2 = \sqrt{\frac{1}{h^2(\pi/2) - h^2(1)} \ln\left[\frac{4J(1)h(1)}{\pi h(\pi/2)}\right]}. \qquad [29]$$

Since the asymptotic expansion has the worst error for small Abs$(m-1)$, all other values of m will produce a better approximation. When the above approximation is used an error of 1% or less is introduced in the calculation.

Table III is a list of the fitting parameters q_1 and q_2 with $h(0)$ and $h(\pi/2)$ for various m.

TABLE III

Table of fitting parameters

m	q_1	q_2	h(0)	$h(\pi/2)$
1.05	-27.9301	31.0506	.320156	05
1.1	-34.0891	16.07096	.458257	.1
1.3	-74.1495	6.02426	.83066	.3
1.3-.01i	-74.0973+2.83337i	6.0187+.169276i	.830750-.0156485i	.3-.01i
1.3-i	74.1207-46.9499 i	1.32201+1.60465 i	1.07434-1.21004 i	.3-i
1.5	-157.782	3.97178	1.118035	.5
1.5-.01i	-157.676+5.89236i	3.97057+.0624025i	1.11807-.013416i	.5-.01i
1.5-.1i	-147.167+57.6607i	3.85538+.601166i	1.12156-.133743i	.5-.1i
1.5-i	155.283-89.3798i	1.48387+1.39853i	1.27679-1.17482i	.5-i
2.0	-987.166	2.37186	1.73205	1
3.0	-34496.5	1.4976	2.82843	2
4.0	-1.12303×10^{6}	1.16944	3.87298	3
5.0	-3.52471×10^{7}	.988750	4.89898	4
6.0	-1.08171×10^{9}	.871188	5.9161	5
7.0	-3.26993×10^{10}	.787146	6.92820	6
8.0	-9.80490×10^{11}	.723318	7.93725	7
9.0	-3.10274×10^{13}	.672757	8.94427	8
10.0	-8.53632×10^{14}	.631446	9.94987	9
100.0	-3.5921×10^{145}	.184026	99.995	99
1000.0	-1.80814×10^{1447}	.057747	999.999	999

Applying the method to [24] with the above information we have:

$$
\begin{aligned}
I_c^1 &\approx \frac{-2q_1q_2}{\sqrt{\pi}} \int_{h(0)}^{h(\pi/2)} \mathrm{H}_1(\lambda_1 h)\, e^{-q_2^2 h^2}\, dh \\
&= \frac{-4q_1q_2\lambda_1^2}{3\pi^{3/2}} \int_{h(0)}^{h(\pi/2)} h^2\, {}_1\mathrm{F}_2\left(\begin{matrix} 1 \\ 3/2, \quad 5/2 \end{matrix} \middle| -\frac{\lambda_1^2 h^2}{4} \right) {}_0\mathrm{F}_0(-q_2^2 h^2)\, dh \\
&= \frac{4q_1q_2\lambda_1^2}{9\pi^{3/2}} \left\{ h^3(0)\, \mathrm{F}_{1:2;0}^{1:1;0}\left[\begin{matrix} 3/2: & 1; \\ 5/2: & 3/2, \quad 5/2; \end{matrix} \middle| \frac{-\lambda_1^2 h^2(0)}{4}, -q_2^2 h^2(0) \right] \right. \\
&\qquad \left. -h^3(\pi/2)\, \mathrm{F}_{1:2;0}^{1:1;0}\left[\begin{matrix} 3/2: & 1; \\ 5/2: & 3/2, \quad 5/2; \end{matrix} \middle| \frac{-\lambda_1^2 h^2(\pi/2)}{4}, -q_2^2 h^2(\pi/2) \right] \right\} \qquad [30]
\end{aligned}
$$

where in the last equation the Kampé de Fériet functions have been reduced from $\mathrm{F}_{2:2;0}^{2:1;0}$ to $\mathrm{F}_{1:2;0}^{1:1;0}$ since a set of coefficients coincided. Simple computer routines for evaluating Kampé de Fériet functions are given in (Ref. 4). These were used in slightly modified form to compute Table IV for small values of s. Other more efficient algorithms for computing [30] are given in Appendix A. These algorithms are derived from the concepts found in Refs. 8 and 9.

Table IV gives errors that are generally less than 10% for real m since the only zero of the integral occurs at $s = 0$ as in Example 1. For complex values of m and sufficiently large values of s, I_c^1 becomes an exponentially increasing function of s. So does the approximation [30]. For any two rapidly increasing functions, a slight displacement in the independent variable of one of the functions will produce a substantial percentage difference between the values of the two functions. Since [30] has a slight difference in phase (i.e., displacement in s) in comparison with I_c^1, large percent errors occur. This can be seen in the error table.

TABLE IV

Error table for Example 3a

m	s	I_c^1 Exact	I_c^1 Approximation	—% Error—
1.1	.5	.0025896	.00223957	13.5
1.1	1	.0103105	.00893241	13.4
1.1	5	.223644	.203632	8.9
1.1	10	.608131	.608241	0.02
1.1	20	.708387	.722618	2.0
1.1	50	.595284	.573136	3.7
1.1-.1i	.5	.00044929-.00501663i	.000147684-.00446461i	67.1,11.0
1.1-.1i	1	.00194818-.0200093i	.000692555-.0178504i	255.5,10.8
1.1-.1i	5	.151968-.444002i	.0974261-.432831i	35.8,2.5
1.3	.5	.0204227	.0190081	6.9
1.3	1	.0793354	.0742178	6.5
1.3	5	.808644	.832955	3.0
1.3	10	.359062	.323648	9.9
1.3	20	.431977	.410225	5.0
1.3	50	.496680	.482361	2.9
1.3-.01i	.5	.0204049-.00126728i	.0189901-.00121746i	6.9,3.9
1.3-.01i	1	.0792763-.00473980i	.0741567-.00463915i	6.5,3.1
1.3-i	.5	-.156730-.157030i	-.162314-.153220i	3.5,2.4
1.3-i	1	-.610466-.861205i	-.652805-.855413i	6.9,0.7
1.3-i	5	1244.224976+951.9054917i	1588.029043+1644.569308i	27.6,72.8
1.5	.5	.0525496	.0502753	4.4
1.5	1	.195683	.188589	3.6
1.5	5	.512050	.503202	1.7
1.5	10	.611504	.626669	2.5
1.5	20	.471594	.499574	5.9
1.5	50	.595284	.573136	3.7
1.5-.01 i	.5	.0525342-.00192994 i	.0502600-.00189406 i	4.3,1.9
1.5-.01 i	1	.195648-.00668855 i	.188554-.00664175 i	3.6,0.7
1.5-.01 i	10	.613522+.011374 i	.611768+.0187999 i	0.3,65.2
1.5-.1 i	.5	.0510075-.0193363i	.0486982-.0189780i	4.5, 1.8
1.5-.1 i	1	.192127-.0672897 i	.184783-.0668288 i	3.8,0.7
1.5-.1 i	5	.4737-.2601 i	.4571-.2974 i	3.5, 14
1.5-i	.5	-.106388-.227092 i	-.122096-.224601 i	14.8,1.1
1.5-i	1	-.218598-1.12719 i	-.254697-1.13575 i	16.5,0.8

TABLE IV (continued)

m	s	I_c^1 Exact	I_c^1 Approximation	--% Error—
2.0	.5	.182774	.179493	1.8
2.0	1	.567054	.562553	2.5
2.0	5	.629007	.640619	1.8
2.0	10	.466074	.488837	4.9
2.0	20	.522300	.527632	1.0
2.0	50	.488015	.492513	0.9
2.0-.1i	.5	.181839-.0318250i	.178535-.0317615i	1.8,0.2
2.0-.1i	1	.569583-.0717892i	.565011-.0730041i	0.8,1.7
5.0	.5	.822542	.824195	0.2
5.0	1	.434339	.470611	8.4
5.0	5	.53203	.547058	2.8
5.0	10	.50478	.507859	0.6
5.0	20	.513551	.490891	4.4
5.0	50	.502995	.500390	0.5

An additional advantage of this technique is that, once the work has been done to find a satisfactory approximation such as [2] and [3], other integrals are readily solved with different $g(u)$ to a similar level of accuracy. For example, if the $\mathbf{H}_1$ function of the above example is changed to a first order Bessel function J_1, the integral [24] becomes:

$$I_c^2 = \int_0^{\pi/2} J_1(\lambda_1 h)\,\sin^2(\theta)\,d\theta. \qquad [31]$$

With the same substitutions as used to obtain the solution to [24] we get:

$$I_c^2 \approx \frac{2q_1q_2}{\sqrt{\pi}} \int_{h(0)}^{h(\pi/2)} J_1(\lambda_1 h)\,e^{-q_3^2h^2}\,dh$$

$$= \frac{2q_1q_2}{\lambda_1\sqrt{\pi}}\left\{e^{-q_2^2h^2(0)}\left[U_2(\frac{i\lambda_1^2}{2q_2^2},\lambda_1h(0)) - iU_1(\frac{i\lambda_1^2}{2q_2^2},\lambda_1h(0))\right]\right.$$
$$\left.-e^{-q_2^2h^2(\pi/2)}\left[U_2(\frac{i\lambda_1^2}{2q_2^2},\lambda_1h(\frac{\pi}{2})) - iU_1(\frac{i\lambda_1^2}{2q_2^2},\lambda_1h(\frac{\pi}{2}))\right]\right\} \quad [32]$$

where U_1 and U_2 are Lommel functions of two variables (Refs. 8 and 10).

Table V is the error table for this approximation. Unlike with $\mathbf{H}_1$, this integral has zeros for real values of m and $s \neq 0$. Thus, the phase problem as previously mentioned in other examples occurs. Again numerical schemes for evaluation of [32] are detailed in Appendix A. For complex m and large s, the large percent errors occur for the same reason as already explained for Table IV.

The quantity of physical interest in cylindrical scattering theory is Q_c, the extinction efficiency. In terms of the above symbols, we have

$$Q_c = 4\mathrm{Re}\left(I_c^2 + iI_c^1\right). \quad [33]$$

This function has no zeros except for $s = 0$. Table VI is an error table of Q_c for complex m. For real m, the percent error is identical to that of Table IV. It is now clearly seen that the errors for complex m are of the same order as for real m even for large s. Furthermore, Q_c approaches 2 for large s and any m, as predicted by Babinet's principle of diffraction from large objects.

TABLE V

Error table for Example 3b

m	s	I_c^2 Exact	I_c^2 Approximation	—% Error—
1.1	.5	.0472756	.0451376	4.5
1.1	1	.0939029	.0898062	4.4
1.1	5	.377706	.378477	0.2
1.1	10	.381027	.413833	8.6
1.1	20	-.126605	-.166460	31.5
1.1	50	-.0425576	-.078062	83.4
1.1-.1i	.5	.0485812-.0453455i	.0459529-.0443288i	5.5,2.2
1.1-.1i	1	.0981060-.0892763i	.0927459-.0876708i	5.5,1.8
1.1-.1i	5	.591899-.217036i	.583436-.265611i	1.4,22.4
1.3	.5	.133658	.130523	2.3
1.3	1	.254182	.249666	0.5
1.3	5	.136981	.150056	9.5
1.3	10	-.0840142	-.0928197	10.5
1.3	20	-.0591054	-.0296963	50.2
1.3	50	-.0376139	-.0206433	54.9
1.3-.01i	.5	.133668-.00410752i	.130533-.00409969i	2.3,0.2
1.3-.01i	1	.254235-.00702857i	.249718-.00711917i	1.8,1.3
1.3-i	.5	.219293-.441338 i	.213943-.446550i	2.4,1.1
1.3-i	1	.912076-1.017280i	.905500-1.05888i	0.7,4.1
1.3-i	5	-951.902855+1243.728089i	-1644.566682+1587.532198i	72.8,27.6
1.5	.5	.211668	.208736	0.3
1.5	1	.371618	.369804	0.5
1.5	5	-.215697	-.241939	12.2
1.5	20	.0528324	.0570300	7.9
1.5	50	.00725979	.00539024	74.2

TABLE V (continued)

m	s	I_c^2 Exact	I_c^2 Approximation	—% Error—
1.5-.01i	.5	.211679-.00368736i	.208748-.00371024i	1.4,0.62
1.5-.01i	1	.371684-.00463889i	.369871-.00480011i	0.48,3.5
1.5-.01i	10	-.0481876+.0211256i	-.0831952+.0205574i	72.6,2.8
1.5-.1i	.5	.212773-.0368971i	.209800-.0371327i	1.5,0.6
1.5-.1i	1	.378135-.0465303i	.37627-.0481714i	0.5,3.5
1.5-.1i	5	-.330915-.0491388i	-.376455-.0628756i	13.8,27.9
1.5-i	.5	.320290-.402570 i	.316487-.407628 i	1.2,1.3
1.5-i	1	1.19943-.643665 i	1.20758-.678831 i	0.7,5.5
2.0	.5	.365144	.363883	0.3
2.0	1	.433180	.438278	1.2
2.0	5	-.0496403	-.0725961	46.2
2.0	10	.0602173	.0729676	21.2
2.0	20	.0274814	.00953082	65.3
2.0	50	-.00742132	.00106124	114.3
2.0-.1i	.5	.366629-.0238937i	.365371-.0242659i	0.3,1.6
2.0-.1i	1	.439381+.0214225i	.444627+.0205887i	1.2,3.9
5.0	.5	-.0866975	-.114949	32.6
5.0	1	.197090	.206872	5.0
5.0	5	.0452478	.0417831	7.7
5.0	10	-.0275163	-.0251509	8.6
5.0	20	.00346559	-.00354774	202.4
5.0	50	-.00472154	-.00248860	52.7

TABLE VI

Error table of Q_c

m	s	Exact	Approximation	—% Error—
1.1-.1i	.5	.1831792	.1779059	2.9
1.1-.1i	1	.3648979	.3534534	3.1
1.1-.1i	5	1.476016	1.452150	1.6
1.3-.01i	.5	.0980497	.0923592	5.8
1.3-.01i	1	.345219	.325103	5.8
1.3-i	.5	1.138432	1.136944	0.1
1.3-i	1	1.627256	1.624300	0.2
1.3-i	5	1.987548	1.987380	.008
1.5-.01i	.5	.224886	.215881	4.0
1.5-.01i	1	.801148	.773416	3.5
1.5-.01i	10	2.369586	2.364842	0.2
1.5-.1i	.5	.351618	.343325	2.4
1.5-.1i	1	.954629	.931818	2.4
1.5-.1i	5	2.09136	2.07990	0.5
1.5-i	.5	1.184728	1.142128	3.6
1.5-i	1	1.700268	1.696536	0.2
2.0-.1i	.5	.8229108	.8112036	1.4
2.0-.1i	1	2.192642	2.177689	0.7

4.0 INTEGRALS INVOLVING THE EXPONENTIAL FUNCTION

In this chapter, we will indicate how this integration technique allows for a trade-off between the complexity of the special function used and the accuracy of the solution. Since several of the examples shown in the last chapter involve integrals over the exponential

function of a complicated argument, we will use this form of integral to demonstrate this point. (It is not coincidental that integrals over the exponential function are common since they are specific cases of general diffraction-type integrals.)

Consider the integral

$$I = \int_a^b e^{h(x)} f(x)\, dx. \qquad [34]$$

The technique then requires

$$I \approx \int_{h(a)}^{h(b)} e^h u(h)\, dh. \qquad [35]$$

If one chooses the form of $u(h)$ to be a polynomial of h with integer powers, the resulting approximation to I will be in terms of a sum of exponential integrals. Thus

$$I \approx \int_{h(a)}^{h(b)} e^h \sum_{k=-n}^{m} a_k h^k\, dh = \sum_{k=-n}^{m} a_k \left(\frac{E_{-k}[h(a)]}{h^{-k-1}(a)} - \frac{E_{-k}[h(b)]}{h^{-k-1}(b)} \right) \qquad [36]$$

where m and n are any positive integers or zero. If we chose $u(h)$ to be a polynomial of h with rational, real or complex powers, then the approximation becomes a series of incomplete gamma functions. Hence,

$$\begin{aligned} I &\approx \int_{h(a)}^{h(b)} e^h \sum_{k=-n}^{m} a_k h^{\mu(k)}\, dh \\ &= \sum_{k=-n}^{m} a_k \left(\Gamma[\mu(k)+1, h(a)] - \Gamma[\mu(k)+1, h(b)] \right) \quad h(a) \text{ and } h(b) \neq 0 \\ &= \sum_{k=0}^{m} a_k \left(\gamma[\mu(k)+1, h(b)] - \gamma[\mu(k)+1, h(a)] \right) \quad \mathrm{Re}[\mu(k)] + 1 > 0. \end{aligned} \qquad [37]$$

Obviously, as one increases the number of terms in the polynomial representation of $u(h)$, the accuracy of the solution will be improved at the cost of adding additional terms. This allows for balancing solution complexity against accuracy.

5.0 CONCLUSIONS AND DISCUSSION

We have developed a method of obtaining an analytic approximation to integrals that may have complicated functions in their kernels. The demonstrated advantages of the technique are:

- sometimes producing a compact, easily calculable form;
- approximations to integrals where standard approaches fail;
- possible trade-offs between functional complexity of the solution against accuracy; and
- solutions that are often globally valid over the full range of each parameter.

Not all of the above advantages may occur when using the technique. When compact forms can be achieved not only can the integral then be rapidly computed but considerable gains in physical insight can follow. Having the ability to compute rapidly, even approximately, difficult integrals is a fundamental requirement in design and inverse problems where parameters have to be varied over large ranges and statistics established for the sensitivity of the results.

We are using this integration technique to solve many integrals involved in the evaluation of the extinction efficiency of randomly oriented discs, infinite cylinders and prolate and oblate spheroids for arbitrary materials and sizes.

Since the form of these integrals is the same as those of general diffraction theory, we expect the technique to be applicable to many problems in optics, as for example the design of Raman cells using exotic laser pumping geometries such as axicons. We also expect the technique to be useful in other fields. It is at this stage a possible solution looking for other promising problems.

6.0 REFERENCES

1. Erdélyi, A., Magnus, W., Oberhettinger, F. and Tricomi, F.G., "Tables of Integral Transforms", Vol. II, McGraw-Hill, New York, 1954.

2. Gradshteyn, I.S. and Ryzhik, I.M., "Table of Integrals, Series, and Products," Academic Press, New York, 1965.

3. Luke, Y.L., "The Special Functions and Their Approximations", Vols. I and II, Academic Press, New York, 1969.

4. Exton, H., "Handbook of Hypergeometric Integrals," Ellis Horwood Ltd., Chichester, England, 1978.

5. Appell, P. and Kampé de Fériet, J., "Fonctions hypergéométriques et hypersphériques. Polynômes d'Hermite," Gautier Villars, Paris, 1926.

6. Fournier, G.R. and Evans, B.T.N., "An Approximation to Extinction Efficiency for Randomly Oriented Spheroids", Applied Optics, Vol. 30, p. 2042, 1991.

7. Stephens, G.L., "Scattering of Plane Waves by Soft Obstacles: Anomalous Diffraction Theory for Circular Cylinders," Applied Optics, Vol. 23, p. 954, 1984.

8. Watson, G.N., "A Treatise on the Theory of Bessel Functions," Cambridge University Press, Cambridge, England, 1945.

9. Agrest, M.M. and Maksimov, M.S., "Theory of Incomplete Cylindrical Functions and their Applications", Springer-Verlag, New York, 1971.

10. Sommargren, G.E. and Weaver, H.J., "Diffraction of Light by an Opaque Sphere. 1: Description and Properties of the Diffraction Pattern", Applied Optics, Vol. 29, p. 4646, 1990.

APPENDIX A

Numerical Schemes for Evaluating Examples 3a and 3b

Evaluating the Fériet functions in [30] and [32] directly as double sums works only if both the arguments are small. If one or both are large, the series will still converge but the intermediate sums will be extremely large. When this occurs, multiprecision calculations would be required for the converged answer to retain any significance. At this point the calculation becomes impractical. Hence other approaches are necessary.

An algorithm that works for small values of $\lambda_1 h$ can be derived from the series expansion for $\mathbf{H}_\nu(z)$ and $J_\nu(z)$ (Ref. 8):

$$\mathbf{H}_\nu(z) + iJ_\nu(z) = \sum_{m=0}^{\infty} \frac{e^{i(1-m)\pi/2}(z/2)^{\nu+m}}{\Gamma(m/2+1)\Gamma(m/2+1+\nu)}. \qquad [A\ 1]$$

Performing the integration as indicated by [30] and [32] on [A 1] term by term with $\nu = 1$ gives:

$$I_c^1 + iI_c^2 = \frac{2q_1q_2}{\sqrt{\pi}}\left\{\frac{h(\pi/2)}{2}\sum_{m=0}^{\infty}\frac{e^{i(1-m)\pi/2}[\lambda_1 h(\pi/2)/2]^{m+1}\gamma^*(m/2+1, q_2^2h^2(\pi/2))}{\Gamma(m/2+2)}\right.$$
$$\left. - \frac{h(0)}{2}\sum_{m=0}^{\infty}\frac{e^{i(1-m)\pi/2}[\lambda_1 h(0)/2]^{m+1}\gamma^*(m/2+1, q_2^2h^2(0))}{\Gamma(m/2+2)}\right\} \qquad [A\ 2]$$

Evidently for m odd, [A 2] gives the expansion for I_c^1 and for m even, the series for I_c^2. It is clear that large $\lambda_1 h$ will create the same summation difficulties as it does for the direct calculation of the Fériet functions. For the case of large $\lambda_1 h$, we can derive an asymptotic series for I_c^1 by a similar term by term integration as was done for [A 2] but over the

asymptotic series for $\mathbf{H}_\nu$ (Ref. 8). Thus taking the asymptotic series

$$\mathbf{H}_\nu(z) \asymp Y_\nu(z) + \frac{1}{\pi}\sum_{k=0}^{m}\frac{\Gamma(k+1/2)}{\Gamma(\nu+1/2-k)(\frac{z}{2})^{2k-\nu+1}} \qquad [A\ 3]$$

we get, again setting $\nu = 1$,

$$I_c^1 \asymp \frac{1}{2} + \frac{2q_1q_2}{\sqrt{\pi}}\left[\frac{h(0)}{\pi}\sum_{k=1}^{n}\frac{\Gamma(k+1/2)E_{k+1/2}[q_2^2h^2(0)]}{\Gamma(3/2-k)[\lambda_1^2h^2(0)]^k}\right.$$

$$\left. - \frac{h(\pi/2)}{\pi}\sum_{k=1}^{n}\frac{\Gamma(k+1/2)E_{k+1/2}[q_2^2h^2(\pi/2)]}{\Gamma(3/2-k)[\lambda_1^2h^2(\pi/2)]^k} + \frac{2q_1q_2}{\sqrt{\pi}}\int_{h(0)}^{h(\pi/2)} Y_1(\lambda_1 h)e^{-q_2^2h^2}dh\right] \qquad [A\ 4]$$

The integral in [A 4] is the same as [32] with Y_1 replaced by J_1. Since the properties of Y_1 and J_1 are very similar, both integrals can be evaluated with a procedure by Agrest and Maksimov (Ref. 9, p.123ff). They develop two series for either J_ν or Y_ν according to whether $2q_2^2h/\lambda_1 \leq 1$ or ≥ 1. In both cases, multiple integration by parts is performed using basic properties of these functions. The details can be found in the cited reference. The results are for J_1:

$$I_c^2 \approx \frac{2q_1q_2}{\sqrt{\pi}\lambda_1}\left\{e^{-q_2^2h^2(0)}\sum_{k=0}^{\infty}\left[\frac{2q_2^2h(0)}{\lambda_1}\right]^k J_k[\lambda_1 h(0)]\right.$$

$$\left. - e^{-q_2^2h^2(\pi/2)}\sum_{k=0}^{\infty}\left[\frac{2q_2^2h(\pi/2)}{\lambda_1}\right]^k J_k[\lambda_1 h(\pi/2)]\right\} \qquad [A\ 5]$$

for $2q_2^2h/\lambda_1 \leq 1$ and

$$I_c^2 \approx \frac{2q_1q_2}{\sqrt{\pi}\lambda_1}\left\{e^{-q_2^2h^2(\pi/2)}\sum_{k=0}^{\infty}\left[\frac{\lambda_1}{2q_2^2h(\pi/2)}\right]^{k+1} J_{-1-k}[\lambda_1 h(\pi/2)]\right.$$

$$\left. - e^{-q_2^2h^2(0)}\sum_{k=0}^{\infty}\left[\frac{\lambda_1}{2q_2^2h(0)}\right]^{k+1} J_{-1-k}[\lambda_1 h(0)]\right\} \qquad [A\ 6]$$

for $2q_2^2h/\lambda_1 \geq 1$,

and letting I_c^3 stand for the analogous case for the integral over Y_1, we get:

$$I_c^3 \approx \frac{2q_1q_2}{\sqrt{\pi}\lambda_1}\left\{e^{-q_2^2h^2(\pi/2)}\sum_{k=0}^{\infty}\left[\frac{2q_2^2h(\pi/2)}{\lambda_1}\right]^k Y_k[\lambda_1 h(\pi/2)]\right.$$
$$\left. -e^{-q_2^2h^2(0)}\sum_{k=0}^{\infty}\left[\frac{2q_2^2h(0)}{\lambda_1}\right]^k Y_k[\lambda_1 h(0)]\right\} \qquad [A\ 7]$$

for $2q_2^2h/\lambda_1 \leq 1$ and

$$I_c^3 \approx \frac{2q_1q_2}{\sqrt{\pi}\lambda_1}\left\{e^{-q_2^2h^2(0)}\sum_{k=0}^{\infty}\left[\frac{\lambda_1}{2q_2^2h(0)}\right]^{k+1} Y_{-1-k}[\lambda_1 h(0)]\right.$$
$$\left. - e^{-q_2^2h^2(\pi/2)}\sum_{k=0}^{\infty}\left[\frac{\lambda_1}{2q_2^2h(\pi/2)}\right]^{k+1} Y_{-1-k}[\lambda_1 h(\pi/2)]\right\} \qquad [A\ 8]$$

for $2q_2^2h/\lambda_1 \geq 1$.

An additional numerical scheme for computing [32] by using the double variable Lommel function representation can be derived from the appendix of Ref. 10.

INTERNAL DISTRIBUTION

DREV R-4653/91

1 - Deputy Chief
1 - Director Electro-optics Division
1 - Director Energetic Materials Division
6 - Document Library
5 - Dr. B.T.N. Evans (author)
1 - Dr. G.R. Fournier (author)
1 - Dr. J. Beaulieu
1 - Dr. P. Pace
1 - Dr. L. Bissonnette
1 - Mr. A. Blanchard
1 - Mr. D. Dion
1 - Mr. R. Carling
1 - Mr. R. Kluchert
1 - Mr. G. Couture
1 - Dr. K. Heaton

EXTERNAL DISTRIBUTION

DREV R-4653/91

2 - DSIS
1 - CRAD
1 - DRDL
1 - DRDM
1 - National Library of Canada
1 - Micromedia Limited
1 - NRC/CISTI
1 - DRIC, U.K.
1 - DTIC, U.S.
1 - DISSLB, Australia

1 - Dr. W.G. Tam
Senior Project Manager
Industrial Research Assistance Program
Laboratory Network
National Research Council
Ottawa, Ontario
K1A 0R6

1 - Dr. A.I. Carswell
Dept. of Physics
York University
4700 Keele Street
North York, Ontario
M3J 1P3

1 - Dr. D. K. Cohoon
West Chester University
Dept. of Mathematics and Computer Science
West Chester, PA 19383
USA

1 - Dr. B.P. Curry
NPB Test Stand
Engineering Physics
Argonne National Laboratory
9700 South Cass Ave., EP/207
Argonne, IL 60439-4841
USA

EXTERNAL DISTRIBUTION (contd)

DREV R-4653/91

1 - Dr. J. Embury
Chemical Research, Development and Engineering Center
SMCRR-RSP-B
Aberdeen Proving Ground, MD 21010-5423
USA

1 - Dr. P. Barber
Clarkson College of Technology
Dept. of Electrical & Computer Engineering
Potsdam, NY 13676
USA

1 - Dr. M. Lax
City College of New York
Physics Dept.
New York, NY 10031
USA

1 - Dr. R.T. Wang
ISST- Space Astronomy Laboratory
1810 NW 6th St.
Gainesville, FL 32609
USA

1 - Dr. G. Kunz
Physics Laboratory of the National Defence
P.O. Box 9 68 64
2509 The Hague
The Netherlands